

Mapping of strongly correlated steady-state nonequilibrium to an effective equilibrium

J. E. Han

Department of Physics, State University of New York at Buffalo, Buffalo, NY 14260, USA

(Dated: September 12, 2018)

By mapping steady-state nonequilibrium to an effective equilibrium, we formulate nonequilibrium problems within an equilibrium picture where we can apply existing equilibrium many-body techniques to steady-state electron transport problems. We study the analytic properties of many-body scattering states, reduce the boundary condition operator in a simple form and prove that this mapping is equivalent to the correct linear-response theory. In an example of infinite- U Anderson impurity model, we approximately solve for the scattering state creation operators, based on which we derive the bias operator \hat{Y} to construct the nonequilibrium ensemble in the form of the Boltzmann factor $e^{-\beta(\hat{H}-\hat{Y})}$. The resulting Hamiltonian is solved by the non-crossing approximation. We obtain the Kondo anomaly conductance at zero bias, inelastic transport via the charge excitation on the quantum dot and significant inelastic current background over a wide range of bias. Finally, we propose a self-consistent algorithm of mapping general steady-state nonequilibrium.

PACS numbers: 73.63.Kv, 72.10.Bg, 72.10.Di

I. INTRODUCTION

Quantum transport theory^{1,2,3} has recently been one of the most exciting fields of condensed matter physics. The field not only has a great promise for providing theoretical framework for the design of nanoscale electronic devices, but also has been a frontier of quantum many-body theory in nonequilibrium.

In regards to predicting behavior of nano-electronic devices the current theories based on non-equilibrium Green function technique^{3,4} have been quite successful. However, as we approach strongly correlated regime of transport^{3,5} under extreme nonequilibrium conditions, approximate Green function techniques become increasingly unreliable. One can make an analogy to the equilibrium quantum statistical mechanics, where the combination of diagrammatic methods and computational techniques has been vital for the great success in the quantum many-body theory during the past decades.

Therefore, it is a pressing issue that we have an alternative theoretical scheme to implement the computational techniques to nonequilibrium problems. Recently new approaches have been proposed to solve nonequilibrium. Mehta and Andrei⁶ have applied the non-equilibrium Bethe Ansatz technique to solve the interacting resonant-level model. Renormalization group theory has been extended to nonequilibrium systems⁷ to investigate the time-dependence⁸.

One of the main problems in applying numerical techniques to transport problems has been the lack of understanding of nonequilibrium ensemble, specifically, as to how nonequilibrium boundary conditions can be implemented as a statistical operator. In steady-state nonequilibrium, Zubarev⁹ has extended the Gibbsian statistical mechanics to incorporate steady-state boundary conditions in the density matrix formalism. Later, Hershfield¹⁰ has shown that the nonequilibrium ensemble can be expressed in the effective Boltzmann factor $e^{-\beta(\hat{H}-\hat{Y})}$ with the bias operator, \hat{Y} , in terms of the scattering state op-

erators. Once the effective Hamiltonian $\hat{H}-\hat{Y}$ inside the Boltzmann factor is obtained, one can use the equilibrium numerical techniques to sample the nonequilibrium ensemble.

Despite the great potential, application of the method has been limited due to the difficulties in constructing the bias operator¹¹. Recently, the method has been implemented by the author¹² in the system of quantum dot (QD) coupled with electron-phonon interaction. In the work, he has approximately constructed the bias operator \hat{Y} by truncating the non-local interaction arising from the nonequilibrium boundary condition and by expanding the scattering state operators up to the harmonic order of the electron-phonon interaction. However, in the strongly correlated limit, such perturbative expansion of the scattering state may not be sufficient to reproduce the many-particle transport such as the Kondo anomaly conductance.

Ultimately, it is desirable that we develop a general computational scheme of mapping nonequilibrium system to an effective equilibrium Hamiltonian, so that equilibrium techniques such as quantum Monte Carlo method can be used to directly calculate nonequilibrium properties. However, to achieve the goal, we must have a good understanding of the properties of the nonequilibrium ensemble. Therefore, in order to gain physical insights of the mapping, we first study the diagrammatic construction of the nonequilibrium ensemble.

The first main goal of this paper is to derive general analytical properties of scattering state operators, especially the anti-commutation and completeness relations in the interacting limit, and derive various expressions of the boundary condition operator. By clarifying the fundamental questions on the properties of scattering state operators, we lay a foundation of the mapping the nonequilibrium. Furthermore, we show that the nonequilibrium mapping produces the correct theory in the zero-bias limit.

The second goal is, by taking an example, to address

what correlation effects have to be included in the bias operator \hat{Y} to properly describe the strongly correlated transport. To this end, we consider the Anderson impurity Hamiltonian as a model for Kondo dot systems. We might expect that, since the original Hamiltonian has a strong on-site interaction, the strong correlation effects will be described simply by shifting chemical potentials in the source, drain reservoirs. However, it will be shown in this work that it is essential to include the correlation effects at the level of Hamiltonian in the boundary condition to produce the Kondo anomaly¹³.

This paper is organized as follows. In Section II, we introduce the idea of mapping the nonequilibrium and present the analytic properties of the scattering state and the bias operators. The proofs are provided in Appendices. In the following Section III-A, we develop a procedure to expand the scattering state operator using the slave-boson representation of the QD states in the infinite on-site Coulomb interaction. We derive expression for the scattering state operators and give physical interpretations in the expansion. In the next subsection III-B, we construct the bias operator \hat{Y} and explain how the nonequilibrium Hamiltonian is calculated in the non-crossing approximation in the equilibrium picture. In the subsection III-C, we derive an approximate expression for the current. In section IV, we present numerical results and discuss strong correlation effects in the differential conductance. In section V, we discuss how the limitations in the previous section can be improved in a self-consistent algorithm.

II. ANALYTIC PROPERTIES OF THE MAPPING

In this section, we discuss the general properties of scattering state operators with many-body interactions present in quantum dot systems and obtain expressions for the bias operator in a simple form. We prove that the zero-bias limit in the mapping of nonequilibrium produces the Kubo formula. The detailed derivations are presented in Appendix.

The general scattering theory has been well-studied and its formalism can be found in many textbooks¹⁴. However, most of them are studied in terms of state vector notation and here we present some of the relations in the operator form. We first consider a quite general model of quantum dot systems. The constraint is that the many-body interaction is confined to the quantum dot. The Lippmann-Schwinger scattering state operator $\psi_{\alpha k \sigma}^\dagger$ is expressed¹⁵ in the operator equation,

$$\psi_{\alpha k \sigma}^\dagger = c_{\alpha k \sigma}^\dagger + \frac{1}{\epsilon_{\alpha k} - \mathcal{L} + i\eta} \mathcal{L}_V c_{\alpha k \sigma}^\dagger, \quad (1)$$

where $c_{\alpha k \sigma}^\dagger$ is the free continuum state creation operator inside the reservoir α at the asymptotic energy $\epsilon_{\alpha k}$ with the continuum index k and spin σ . η is a infinitesimal positive number to define the asymptotic limit of the

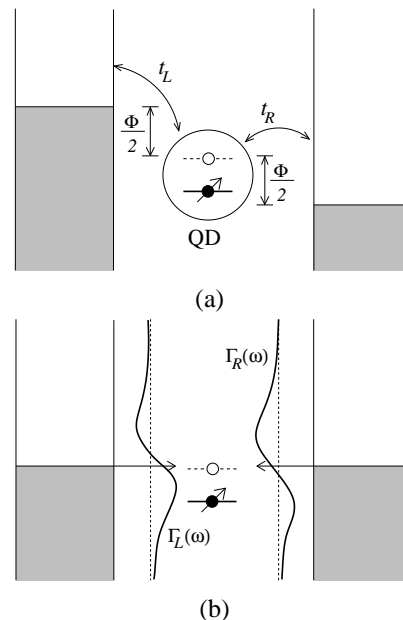


FIG. 1: (a) Schematic energy diagram with chemical potential bias Φ applied between the source and drain reservoirs. The empty level of the quantum dot is aligned at the middle of the two chemical potentials. (b) After the mapping of steady-state nonequilibrium to an effective equilibrium via the boundary condition operator \hat{Y} , the energy diagram of $\hat{H} - \hat{Y}$ has equal chemical potential. The non-zero current is recovered in the modified hybridization functions (solid curves) between the QD and the reservoirs.

scattering state.¹⁵ Here the Liouville operators for the full Hamiltonian \mathcal{L} and the interaction \mathcal{L}_V are defined in the commutation relation such as $\mathcal{L}\hat{A} = [\hat{H}, \hat{A}]$ for any operator. The $\alpha (= \pm)$ index refers to the reservoir [$+ \leftrightarrow$ source reservoir (L), $- \leftrightarrow$ drain reservoir (R)].

Since the Hamiltonian has many-body interactions, the scattering state operator ψ^\dagger has terms with many-particle operators, and it is not clear if they obey the regular fermion anti-commutation relation. In non-interacting models, it can be shown straightforwardly that the anti-commutation relation holds. It is shown in Appendix A that the following commutation relation holds even in the interacting limit:

$$\{\psi_{\alpha k \sigma}^\dagger, \psi_{\alpha' k' \sigma'}\} = \delta_{\alpha \alpha'} \delta_{k k'} \delta_{\sigma \sigma'}. \quad (2)$$

Therefore, ψ^\dagger, ψ work like typical fermion operators and any scattering state created by repeated application of ψ^\dagger 's on a particle-vacuum can be considered a many-body scattering state.

One of the obstacles in implementing the mapping of nonequilibrium has been the lack of understanding of the bias condition operator suggested by Hershfield¹⁰,

$$\hat{Y} = \frac{\Phi}{2} \sum_{k\sigma} \left(\psi_{Lk\sigma}^\dagger \psi_{Lk\sigma} - \psi_{Rk\sigma}^\dagger \psi_{Rk\sigma} \right). \quad (3)$$

We reduce the \hat{Y} operator in a physically appealing form

in Appendix B as

$$\hat{Y} = \Phi \left[\frac{1}{2} \sum_{\alpha k \sigma} \alpha c_{\alpha k \sigma}^\dagger c_{\alpha k \sigma} - \frac{1}{e - \mathcal{L} + i\eta} \hat{I} \right], \quad (4)$$

with the current operator \hat{I} which will be defined later. Although the bias operator has been derived from the boundary condition imposed with respect to the chemical potential difference, the above formula relates the potential-driven ensemble to a current-driven ensemble¹⁶.

Expressing the bias operator in terms of current operator becomes particularly useful in proving the zero-bias limit of the conductance. The formulation of nonequilibrium mapping via \hat{Y} must produce the same Kubo formula in equilibrium theory. The proof in Appendix C shows that the mapping of nonequilibrium has the correct description of transport physics in the low-bias limit. So far, the present formulation of nonequilibrium has been shown to be correct in the non-interacting models at finite bias¹² and in the interacting models in the zero-bias limit.

The notion that we can treat the scattering states as independent dynamical degrees of freedom has been the central idea in the mapping of nonequilibrium. In the non-interacting model¹², the scattering state operators are on a firm ground due to the anti-commutation relation mentioned above and the completeness of the scattering states encapsulated in the following identity

$$\sum_{\alpha k \sigma} \psi_{\alpha k \sigma}^\dagger \psi_{\alpha k \sigma} = \sum_{\alpha k \sigma} c_{\alpha k \sigma}^\dagger c_{\alpha k \sigma} + \sum_{\sigma} d_{\sigma}^\dagger d_{\sigma}, \quad (5)$$

provided that there exist no bound states, which is the case in the limit of large bandwidth. In the interacting systems, the scattering state operators $\psi_{\alpha k \sigma}^\dagger$ become dressed with multi-particle scattering. Therefore, $\psi_{\alpha k \sigma}^\dagger$ should be defined in the many-particle basis and the validity of the above equation is not obvious. In Appendix D, we derive the relation for a fairly general class of interactions.

Similarly, behind the idea of writing the bias operator \hat{Y} by shifting the chemical potential of $\psi_{\alpha k \sigma}^\dagger$, we expect for a consistent theory that

$$\hat{H} - \hat{Y} = \sum_{\alpha k \sigma} (\epsilon_{\alpha k \sigma} - \alpha \Phi / 2) \psi_{\alpha k \sigma}^\dagger \psi_{\alpha k \sigma}, \quad (6)$$

and therefore

$$\hat{H} = \sum_{\alpha k \sigma} \epsilon_{\alpha k \sigma} \psi_{\alpha k \sigma}^\dagger \psi_{\alpha k \sigma}. \quad (7)$$

We derive a general relation for the above summation in Appendix D and explicitly demonstrate that the relation Eq. (7) holds for the Anderson impurity model. This relation corresponds to the intertwining relation in the S -matrix formalism in the absence of bound states. Even if the products $\psi_{\alpha k \sigma}^\dagger \psi_{\alpha k \sigma}$ has a quadratic form,

they contain many-body interactions to infinite orders in the original basis. However, after the summation over all $(\alpha k \sigma)$ indices, only finite order terms up to the original Hamiltonian survive.

III. NONEQUILIBRIUM IN ANDERSON IMPURITY MODEL

For the remainder of this paper until Section V, we will consider an example of electron transport in the infinite- U Anderson model as a model for strongly correlated transport system. In such systems where local interaction dominates the electronic structure, it is natural to choose the local states as the unperturbed states. One of the very successful and popular methods is the slave-boson technique, often used in the limit of infinite interaction strength. In our model, by letting the on-site Coulomb interaction to be infinite, we effectively project out the Hilbert space associated with d^2 QD states. Therefore the available local Hilbert space is $\{|0\rangle, |d_\sigma\rangle : \sigma = 1, \dots, N\}$, constrained by the relation

$$|0\rangle\langle 0| + \sum_{\sigma=1}^N |d_\sigma\rangle\langle d_\sigma| = 1. \quad (8)$$

Due to the truncation of the Hilbert space, the QD states $|d_\sigma\rangle$ cannot be represented by ordinary fermion operators. One of the techniques to overcome this problem is the slave-boson method, where we associate the empty state $|0\rangle$ by a bosonic state $b^\dagger|vac\rangle$, created by a slave-boson creation operator b^\dagger on an imaginary vacuum $|vac\rangle$ and the singly-occupied states $|d_\sigma\rangle$ by $f_\sigma^\dagger|vac\rangle$ with pseudo-fermion operator f_σ^\dagger . The above constraint can be now recast in the following operator relation,

$$b^\dagger b + \sum_{\sigma=1}^N f_\sigma^\dagger f_\sigma = 1. \quad (9)$$

Under the assumption of the above projection, the Hamiltonian can be written in terms of fermion-boson operators as

$$\hat{H} = \hat{H}_0 + \hat{V} \quad (10)$$

$$\hat{H}_0 = \sum_{\alpha k \sigma} \epsilon_{\alpha k} c_{\alpha k \sigma}^\dagger c_{\alpha k \sigma} + \epsilon_d \sum_{\sigma} f_\sigma^\dagger f_\sigma \quad (11)$$

$$\hat{V} = \sum_{\alpha k \sigma} \frac{t_{\alpha k \sigma}}{\sqrt{\Omega}} \left(b f_\sigma^\dagger c_{\alpha k \sigma} + c_{\alpha k \sigma}^\dagger f_\sigma b^\dagger \right), \quad (12)$$

with the QD level energy ϵ_d , tunneling amplitude $t_{\alpha k \sigma}$ and the volume factor Ω . The unperturbed Hamiltonian \hat{H}_0 has the reservoir continua and local basis as disconnected. The perturbation term \hat{V} turns on the tunneling between the reservoirs and the quantum dot.

Since the steady-state ensemble must be time-independent, we construct the nonequilibrium boundary

condition in terms of the scattering states¹⁰. The scattering state creation operator $\psi_{\alpha k \sigma}^\dagger$ can be written in the Lippmann-Schwinger equation^{9,15,17}:

$$\psi_{\alpha k \sigma}^\dagger = c_{\alpha k \sigma}^\dagger + \frac{1}{\epsilon_{\alpha k} - \mathcal{L}_0 + i\eta} \mathcal{L}_V \psi_{\alpha k \sigma}^\dagger, \quad (13)$$

with the Liouville operator \mathcal{L}_0 with respect to \hat{H}_0 defined as $\mathcal{L}_0 \hat{A} = [\hat{H}_0, \hat{A}]$ for an arbitrary operator \hat{A} , and similarly $\mathcal{L}_V \hat{A} = [\hat{V}, \hat{A}]$. This formula is equivalent to Eq. (1). The scattering state operator is expanded in a perturbation series of the tunneling part \mathcal{L}_V ,

$$\begin{aligned} \psi_{\alpha k \sigma}^\dagger &= c_{\alpha k \sigma}^\dagger + \sum_{n=1}^{\infty} \psi_{n, \alpha k \sigma}^\dagger \\ &= c_{\alpha k \sigma}^\dagger + \sum_{n=1}^{\infty} \left(\frac{1}{\epsilon_{\alpha k} - \mathcal{L}_0 + i\eta} \mathcal{L}_V \right)^n c_{\alpha k \sigma}^\dagger. \end{aligned} \quad (14)$$

The n -th order term can be derived recursively as

$$\psi_{n, \alpha k \sigma}^\dagger = \frac{1}{\epsilon_{\alpha k} - \mathcal{L}_0 + i\eta} \mathcal{L}_V \psi_{n-1, \alpha k \sigma}^\dagger. \quad (15)$$

The statistical operator \hat{Y} for the nonequilibrium boundary condition is defined as in Eq. (3).

If the interaction is local, one can easily see that the scattered part of the wave-function, $\Delta \psi_{\alpha k \sigma}^\dagger = \sum_n \psi_{n, \alpha k \sigma}^\dagger$, has the k -dependence only through $\epsilon_{\alpha k}$. To eliminate unnecessary band-edge effects and bound states, we consider a infinite band Lorentzian density of states (DOS)¹⁸ for the both reservoirs $N_\alpha(\epsilon) = (D/\pi)(\epsilon^2 + D^2)^{-1}$ with the half-bandwidth D . Then at $\epsilon_{Lk} = \epsilon_{Rk'}$ we have $\Delta \psi_{Lk\sigma}^\dagger = \Delta \psi_{Rk'\sigma}^\dagger$. After the k -summation with the DOS of broad bandwidth and by assuming the symmetric source-drain parameters, we have a cancellation between $\Delta \psi_{Lk\sigma}^\dagger \Delta \psi_{Lk\sigma}$ and $\Delta \psi_{Rk\sigma}^\dagger \Delta \psi_{Rk\sigma}$ in \hat{Y} :

$$\hat{Y} = \hat{Y}_0 + \frac{\Phi}{2} \sum_{k\sigma} \left(\Delta \psi_{Lk\sigma}^\dagger c_{Lk\sigma} - \Delta \psi_{Rk'\sigma}^\dagger c_{Rk'\sigma} + h.c. \right), \quad (16)$$

with $\hat{Y}_0 = (\Phi/2) \sum_{k\sigma} (c_{Lk\sigma}^\dagger c_{Lk\sigma} - c_{Rk\sigma}^\dagger c_{Rk\sigma})$.

A. Expansion of $\psi_{\alpha k \sigma}^\dagger$

We expand the scattering state operator $\psi_{\alpha k \sigma}^\dagger$ as depicted in FIG. 2. FIG. 2(a) shows the diagram for the $n = 1$ contribution. The solid line is for the conduction electron, the dashed line for the pseudo-fermion f_σ and the wavy line for the slave-boson b .

$$\psi_{1, \alpha k \sigma}^\dagger = \frac{1}{\epsilon_{\alpha k} - \mathcal{L}_0 + i\eta} \mathcal{L}_V c_{\alpha k \sigma}^\dagger = \frac{t_\alpha}{\sqrt{\Omega}} \frac{b f_\sigma^\dagger}{\epsilon_{\alpha k} - \epsilon_d + i\eta}. \quad (17)$$

From now on, we use a shorthand notation $q \equiv (\alpha k)$. As mentioned above, we assume the left-right symmetry

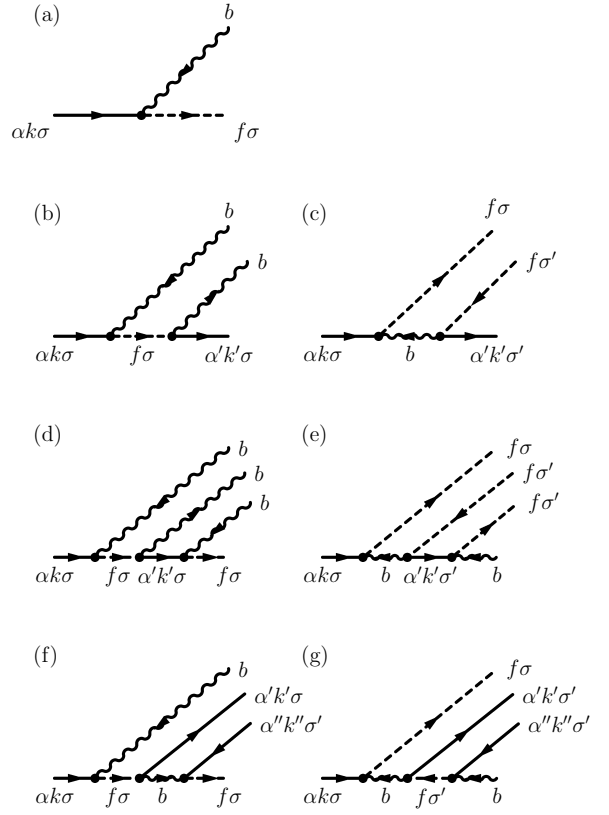


FIG. 2: Diagrams in the expansion of the scattering state operator $\psi_{\alpha k \sigma}^\dagger$, expanded perturbatively with respect to the tunneling term \hat{V} in the infinite- U Anderson impurity model.

and the tunneling amplitudes are independent of k , i.e., $t_q = t$.

In the $n = 2$ term, we first compute $\mathcal{L}_V(b f_\sigma^\dagger)$ as

$$\mathcal{L}_V(b f_\sigma^\dagger) = \sum_{q'\sigma'} \frac{t_{q'}}{\sqrt{\Omega}} c_{q'\sigma'}^\dagger (\delta_{\sigma\sigma'} + b^\dagger b \delta_{\sigma\sigma'} - f_{\sigma'} f_\sigma^\dagger), \quad (18)$$

where $b^2 = 0$ has been used in the above calculation since any physical state subject to the constraint Eq. (9) is projected out by the application of b^2 operator. Therefore,

$$\psi_{2, q\sigma}^\dagger = \sum_{q'\sigma'} \frac{t_{q'}^2}{\Omega} \frac{c_{q'\sigma'}^\dagger (\delta_{\sigma\sigma'} + b^\dagger b \delta_{\sigma\sigma'} - f_{\sigma'} f_\sigma^\dagger)}{(\epsilon_q - \epsilon_{q'} + i\eta)(\epsilon_q - \epsilon_d + i\eta)}. \quad (19)$$

The second term in the parenthesis of the numerator corresponds to the diagram in FIG. 2(b) and the third term to (c).

The third order term ($n = 3$) is obtained from $\psi_{3, q\sigma}^\dagger = (\epsilon_{\alpha k} - \mathcal{L}_0 + i\eta)^{-1} \mathcal{L}_V \psi_{2, q\sigma}^\dagger$. We have simplified the algebra of commutation relations regarding the QD operators by imposing the constraint Eq. (9), such as $bb^\dagger b = b$ and $b f_{\sigma'}^\dagger f_{\sigma'} f_\sigma^\dagger = b f_\sigma^\dagger \delta_{\sigma\sigma'}$. With regards to the conduction electron operators, we ignore the off-diagonal density and

electron (hole) pair operators as

$$c_{q''\sigma''}c_{q'\sigma'}^\dagger \approx c_{q'\sigma'}c_{q''\sigma''}^\dagger \delta_{q'q''} \delta_{\sigma'\sigma''} \quad (20)$$

$$c_{q\sigma}^\dagger c_{q'\sigma'}^\dagger, c_{q\sigma} c_{q'\sigma'} \approx 0. \quad (21)$$

If we do not consider any effects on transport from spontaneous magnetic ordering in the continuum states, *i.e.* $\langle c_{\alpha k\sigma}^\dagger c_{\alpha'k'\sigma} \rangle = 0$, or pairing correlation, *i.e.* $\langle c_{\alpha k\sigma}^\dagger c_{\alpha'k'\sigma'}^\dagger \rangle = 0$, it is reasonable to drop the corresponding operator products.

Justification of the $q' = q''$ condition seems less obvious. We discuss this in conjunction with the $U = \infty$ condition¹⁹ as follows. As will be discussed below, we will replace the operator product $c_{q'\sigma'}^\dagger c_{q''\sigma''}$ by its expectation value, which amounts to contracting the out-going electron-hole lines in FIG. 2 (f-g). However, if $q' \neq q''$ there must be a slave-boson-fermion loop to mediate the off-diagonal conduction electron states. This contributes to an extra-charge Q number in the Coleman's formulation¹⁹ of the infinite- U model and can be projected out. It can be argued that the outgoing conduction electron line will be eventually contracted in higher order diagrams. However, that corresponds to the so-called crossing-diagrams²⁰ which are of higher order in $1/N$ and negligible in the large N limit. Therefore, in the context of the large- U and large- N limit, the off-diagonal density operators are ignored.

With above approximations, the third order contribution of the scattering state operator becomes

$$\psi_{3,q\sigma}^\dagger = \frac{t_\alpha/\sqrt{\Omega}}{(\epsilon_q - \epsilon_d + i\eta)^2} \left(-i\Gamma + \hat{\Sigma}_r(\epsilon_q) \right) b f_\sigma^\dagger, \quad (22)$$

where $\Gamma = \Gamma_L + \Gamma_R$, $\Gamma_\alpha = \Omega^{-1}\pi t^2 \sum_k \delta(\epsilon - \epsilon_{\alpha k}) = \pi t^2 N(0)$ with $N(0)$ the density of states of the reservoirs. The retarded self-energy operator is defined as

$$\hat{\Sigma}_r(\epsilon) = \frac{t_\alpha^2}{\Omega} \sum_{q',\sigma' \neq \sigma} \frac{c_{q'\sigma'}^\dagger c_{q'\sigma'}}{\epsilon_q - \epsilon_{q'} + i\eta}. \quad (23)$$

Applying the same approximations discussed above, we obtain higher order perturbation terms in a geometric series as

$$\begin{aligned} \psi_{\text{odd},q\sigma}^\dagger &= \sum_{n=1,3,\dots,\infty} \psi_{n,q\sigma}^\dagger \quad (24) \\ &= \frac{t_\alpha}{\sqrt{\Omega}} b f_\sigma^\dagger \left(\epsilon_{\alpha k} - \epsilon_d + i\Gamma - \hat{\Sigma}_r(\epsilon_q) \right)^{-1}. \quad (25) \end{aligned}$$

So far the self-energy *operator* is derived from the equation of motion and is independent of the boundary condition.

Here we replace the pairs of electron operators in the numerator of the self-energy operator with average values in the asymptotic limit, $c_{q,\sigma}^\dagger c_{q\sigma} \approx \langle \psi_{\alpha k\sigma}^\dagger \psi_{\alpha k\sigma} \rangle = f(\epsilon_{\alpha k} - \alpha\Phi/2) \equiv f_\alpha(\epsilon_{\alpha k})$, with the Fermi-Dirac function $f(\epsilon) = (1 + e^{\beta\epsilon})^{-1}$. The different chemical potential

of the source-drain reservoirs is taken into account in the $\alpha\Phi/2$ term. By taking the expectation value over the self-energy operator, we have incorporated the boundary condition in the scattering state. We define an effective retarded Green function $g_d(\epsilon) = [\epsilon_{\alpha k} - \epsilon_d + i\Gamma - \Sigma^r(\epsilon_q)]^{-1}$ in terms of the retarded self-energy $\Sigma^r(\epsilon)$ given as

$$\begin{aligned} \Sigma^r(\epsilon_q) &= \frac{1}{\Omega} \sum_{q'\sigma' \neq \sigma} \frac{t_\alpha^2 f_{\alpha'}(\epsilon_{q'})}{\epsilon_q - \epsilon_{q'} + i\eta} \\ &= (N-1) \sum_{\alpha'} \frac{\Gamma_{\alpha'}}{\pi} \int d\epsilon' \frac{n_{\alpha'}(\epsilon') f_{\alpha'}(\epsilon')}{\epsilon_q - \epsilon' + i\eta}, \quad (26) \end{aligned}$$

with the renormalized DOS for the α -th reservoir $n_{\alpha'}(\epsilon') = N_{\alpha'}(\epsilon')/N_{\alpha'}(0)$. The self-energy $\Sigma^r(\epsilon)$ has a logarithmic singularity in the limit of $T = 0$ for $\epsilon_q \rightarrow \alpha\Phi/2$ as

$$\begin{aligned} &\int d\epsilon' \frac{n_{\alpha'}(\epsilon') f_{\alpha'}(\epsilon')}{\epsilon_q - \epsilon' + i\eta} \\ &\approx \ln \frac{1}{|\epsilon_q - \alpha\Phi/2|} - i\pi n_{\alpha'}(\epsilon_q) \theta(\alpha\Phi/2 - \epsilon_q). \quad (27) \end{aligned}$$

This has the familiar form of the Brillouine-Wigner perturbation theory²⁰ and goes back to the typical expression in the zero-bias limit (with a single chemical potential). We now write the odd-order perturbation terms of the scattering state operator as

$$\Delta\psi_{\text{odd},q\sigma}^\dagger = \frac{t}{\sqrt{\Omega}} g_d(\epsilon_q) b f_\sigma^\dagger, \quad (28)$$

which has the same form as in the non-interacting resonant level QD system when $g_d(\epsilon_q)$ is replaced with the non-interacting function¹² $(\epsilon_{\alpha k} - \epsilon_d + i\Gamma)^{-1}$. The renormalization factor due to $\Sigma^r(\epsilon)$ is essential to construct the bias operator \hat{Y} in the strongly correlated limit. As will be shown later, anomalous Kondo peak at zero bias cannot be produced without this logarithmic singularity.

The approximations used here are motivated to produce physically intuitive formula, similar to the scattering states in the non-interacting limit. We view that the many-body particle terms in the scattering state operators as out-going single particle states dressed with contractible many-particle excitations. One can interpret the replacement of many-particle operators by single-particle operators with renormalized amplitude as a quasi-particle approximation, in the similar spirit of the Fermi-liquid theory.

The even order perturbation terms can be obtained from $\Delta\psi_{\text{even},q\sigma}^\dagger = (\epsilon_q - \mathcal{L}_0 + i\eta)^{-1} \mathcal{L}_V \Delta\psi_{\text{odd},q\sigma}^\dagger$ and, using the approximations leading to Eq. (28), we get

$$\Delta\psi_{\text{even},q\sigma}^\dagger = \frac{t^2}{\Omega} \sum_{q'\sigma'} \frac{g_d(\epsilon_q)}{\epsilon_q - \epsilon_{q'} + i\eta} c_{q'\sigma'}^\dagger (\delta_{\sigma\sigma'} + b^\dagger b \delta_{\sigma\sigma'} - f_{\sigma'} f_\sigma^\dagger), \quad (29)$$

which can be interpreted as the renormalized scattered wave. Finally the approximate scattering state operator

is

$$\begin{aligned} \psi_{q\sigma}^\dagger &= c_{q\sigma}^\dagger + \frac{t}{\sqrt{\Omega}} g_d(\epsilon_q) b f_\sigma^\dagger \\ &+ \frac{t^2}{\Omega} \sum_{q'\sigma'} \frac{g_d(\epsilon_q)}{\epsilon_q - \epsilon_{q'} + i\eta} c_{q'\sigma'}^\dagger (\delta_{\sigma\sigma'} + b^\dagger b \delta_{\sigma\sigma'} - f_{\sigma'}^\dagger f_\sigma^\dagger), \end{aligned} \quad (30)$$

which has the similar structure of the non-interacting scattering state.

The physical meaning of the above scattering state is quite transparent. The second term is for the conduction electrons to tunnel on to the QD site with the amplitude given by the full Green function. The last term involving continuum states is either from the potential scattering or from the exchange of the conduction with the QD electrons. Due to the approximation of $U = \infty$, local electrons first tunnel out to the reservoir and the empty local state is subsequently filled by a conduction electron from the reservoir ($d^1 \rightarrow d^0 \rightarrow d^1$).

If the outgoing conduction electron were to be in the same spin state as the incoming spin, there are two possibilities. First, when the initial QD is in the empty state $b^\dagger|vac\rangle$, a conduction electron goes through the potential scattering to hop onto the QD and then tunnels out with the same spin ($d^0 \rightarrow d^1 \rightarrow d^0$). It can be seen explicitly from Eq. (31) that the initially empty QD state ($b^\dagger|vac\rangle$) does not change after the scattering $[(\delta_{\sigma\sigma'} + b^\dagger b \delta_{\sigma\sigma'} - f_{\sigma'}^\dagger f_\sigma^\dagger) b^\dagger|vac\rangle = \delta_{\sigma\sigma'} b^\dagger|vac\rangle]$. Second, if the QD was singly occupied with the same spin as the incoming state ($f_\sigma^\dagger|vac\rangle$), the QD electron exchanges with the incoming electron without flipping the spin, $[(1 + b^\dagger b - f_\sigma f_\sigma^\dagger) f_\sigma^\dagger|vac\rangle = f_\sigma^\dagger|vac\rangle]$. Therefore, when the incoming and out-going waves have the same spin, the factor $(\delta_{\sigma\sigma'} + b^\dagger b \delta_{\sigma\sigma'} - f_{\sigma'}^\dagger f_\sigma^\dagger)$ can be considered as one.

However, if the QD had a different spin state ($f_{\sigma'}^\dagger|vac\rangle$, $\sigma' \neq \sigma$) from the incoming electron, the outgoing electron cannot be in the same spin state as the incoming one $[(1 + b^\dagger b - f_\sigma f_\sigma^\dagger) f_{\sigma'}^\dagger|vac\rangle = 0]$, since d^2 -configurations are forbidden by the $U = \infty$ condition and therefore the QD electron must hop out first in a scattering event.

B. Effective Hamiltonian and Non-crossing Approximation

Here, we focus on how the reservoir-QD tunneling is modified by the bias. The modified tunneling results from the second term in Eq. (31), and the bias operator Eq. (16) is written as

$$\begin{aligned} \hat{Y} &= \frac{\Phi}{2} \sum_{\alpha k} \alpha \left[c_{\alpha k \sigma}^\dagger c_{\alpha k \sigma} + \frac{t}{\sqrt{\Omega}} g_d(\epsilon_{\alpha k}) b f_\sigma^\dagger c_{\alpha k \sigma} + h.c. \right] \\ &+ \hat{Y}_{cc}, \end{aligned} \quad (31)$$

where the last term \hat{Y}_{cc} accounts for the non-diagonal coupling between conduction electrons, proportional to

$c_{\alpha k \sigma}^\dagger c_{\alpha' k' \sigma'}$, created by the steady-state boundary condition. Finally an approximate effective nonequilibrium Hamiltonian $\hat{\mathcal{H}} = \hat{H} - \hat{Y}$ becomes

$$\begin{aligned} \hat{\mathcal{H}} &= \hat{H} - \hat{Y} \\ &= \sum_{\alpha k \sigma} \left[\epsilon_{\alpha k} - \frac{\alpha \Phi}{2} \right] c_{\alpha k \sigma}^\dagger c_{\alpha k \sigma} + \epsilon_d \sum_{\sigma} f_\sigma^\dagger f_\sigma \\ &+ \frac{t}{\sqrt{\Omega}} \sum_{\alpha k \sigma} \left[\left(1 - \frac{\alpha \Phi}{2} g_d(\epsilon_{\alpha k}) \right) b f_\sigma^\dagger c_{\alpha k \sigma} + h.c. \right] - \hat{Y}_{cc}. \end{aligned} \quad (32)$$

Since the scattering state Eq. (31) is an extended state, the product of $\psi_{q\sigma}^\dagger \psi_{q\sigma}$ in \hat{Y} produces non-local interaction between all possible basis states and Hamiltonians with only local interaction become non-local after the mapping. Usually we need a truncation scheme to treat the non-locality¹². In the above Hamiltonian, the non-local effects are implicitly included in the modified tunneling and we do not consider additional non-local effects in this work.

In this section, we calculate the the on-site QD Green function $\mathcal{G}_d(\omega)$. Since the non-local terms in Y_{cc} have indirect effects to $\mathcal{G}_d(\omega)$, we temporarily drop Y_{cc} in the calculation of $\mathcal{G}_d(\omega)$. We use curly symbols, such as $\hat{\mathcal{H}}$ and $\mathcal{G}_d(\omega)$, to denote the quantities which are derived with $\hat{H} - \hat{Y}$ as the time-evolution generator.

To solve the effective Hamiltonian subject to the constraint condition Eq. (9), we use the Coleman's projection method¹⁹ and perform the nonperturbative partial summation of Feynman diagrams in the non-crossing approximation (NCA)²⁰. The constraint condition is imposed within the grand-canonical ensemble scheme with respect to the quantum dot charge operator \hat{Q} defined as $\hat{Q} = b^\dagger b + \sum_{\sigma} f_\sigma^\dagger f_\sigma$. Only the subspace Q_1 (with $\hat{Q} = 1$) is physically meaningful. The grand-canonical ensemble is introduced with a fictitious chemical potential $-\lambda$ associated with \hat{Q} in the partition function $Z_G(\lambda)$ as

$$Z_G(\lambda) = \text{Tr} e^{-\beta(\hat{\mathcal{H}} + \lambda \hat{Q})} = \sum_{Q=0}^{\infty} Z_c(Q) e^{-\beta \lambda Q}, \quad (33)$$

with the partition function $Z_c(Q)$ in the subspace of the fixed charge $\hat{Q} = Q$. The expectation value of an operator \hat{A} averaged over $Z_c(Q = 1)$ is accomplished by taking the $\lambda \rightarrow \infty$ limit as

$$\langle \hat{A} \rangle = \lim_{\lambda \rightarrow \infty} \frac{\langle \hat{A} \hat{Q} \rangle_\lambda}{\langle \hat{Q} \rangle_\lambda}, \quad (34)$$

where the average $\langle \dots \rangle_\lambda$ is taken over the grand-canonical ensemble before λ is taken to the infinity and regular Feynman diagram technique can be applied to evaluate the average.

Feynman diagrams are partially summed by treating the inverse of the QD degeneracy, $1/N$, as the expansion parameter. The non-crossing approximation exploits the fact that diagrams with crossing one-particle propagators contribute to the high order expansion in $O(1/N^2)$, and

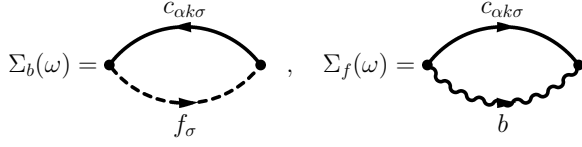


FIG. 3: Non-crossing approximation diagrams for the self-energies of slave-boson (b) and pseudo-fermion (f_σ).

therefore can be ignored in the limit of large QD degeneracy. This procedure can be summed up in the self-energy diagrams depicted in FIG. 3. The dashed line represents the *full* Green function for the pseudo-fermion, the wavy line for the slave-boson, and the solid line for the bare conduction electron. After $\lambda \rightarrow \infty$ limit is taken, the self-energies $\Sigma_b(\omega), \Sigma_f(\omega)$ for b, f_σ can be expressed as

$$\Sigma_b(\omega) = N \sum_{\alpha=\pm} \int d\epsilon \frac{\tilde{\Gamma}_\alpha(\epsilon)}{\pi} f_\alpha(\epsilon) G_f(\omega + \epsilon'_\alpha) \quad (35)$$

$$\Sigma_f(\omega) = \sum_{\alpha=\pm} \int d\epsilon \frac{\tilde{\Gamma}_\alpha(\epsilon)}{\pi} [1 - f_\alpha(\epsilon)] G_b(\omega - \epsilon'_\alpha), \quad (36)$$

with $\epsilon'_\alpha = \epsilon - \alpha\Phi/2$. $G_b(\omega), G_f(\omega)$ are full one-particle Green functions for the slave-boson and pseudo-fermion, respectively, defined as

$$G_b(\omega) = [\omega - \Sigma_b(\omega)]^{-1} \quad (37)$$

$$G_f(\omega) = [\omega - \epsilon_d - \Sigma_f(\omega)]^{-1}. \quad (38)$$

The effective hybridization function $\tilde{\Gamma}_\alpha(\epsilon)$ is defined with the modified tunneling amplitude in Eq. (32) as

$$\tilde{\Gamma}_\alpha(\epsilon) = \pi t^2 \left| 1 - \frac{\alpha\Phi}{2} g_d(\epsilon) \right|^2 N_\alpha(\epsilon). \quad (39)$$

The closed set of Eqs. (35-39) is self-consistently solved.

The shifted continuum energy levels and the effective hybridization function in $\hat{\mathcal{H}}$ is schematically sketched in FIG. 1(b). The dashed line is the original hybridization function at zero bias with a flat DOS. As the bias Φ is turned on, the hybridization is modified by the term proportional to $\Phi g_d(\epsilon)$ in Eq. (39), as drawn in solid line. The enhancement of the effective hybridization from the source reservoir $\Gamma_L(\omega)$ at lower energy can be understood as follows. The bias voltage creates a current-carrying nonequilibrium ensemble. However, after adjusting the chemical potentials of the two reservoirs to the same level, the electron current ($L \rightarrow R$) should be restored via the effective tunneling. By enhancing the tunneling magnitude, hence the hybridization, to the source reservoir and suppressing the drain-hybridization for the low energy states, we recover the electron flow from L to R . Similarly, the enhanced drain-hybridization at higher energy promotes the hole-current from R to L . In fact, it is not only the magnitude of the tunneling parameters but also the phase factor (coming from the retarded Green function) associated with the tunneling electrons which

contribute to the current. This phase factor breaks the time-reversal symmetry.

The on-site Green function of the QD state, $\mathcal{G}_d(\omega)$, can be expressed as a convoluted integral of $b - f$ spectral functions as

$$\mathcal{G}_d(\omega) = \int d\epsilon \frac{\rho_d(\epsilon)}{\omega - \epsilon + i\eta}, \quad (40)$$

with its spectral function $\rho_d(\epsilon)$ given as

$$\rho_d(\epsilon) = \frac{1 + e^{-\beta\epsilon}}{Z_f} \int d\epsilon' \rho_b(\epsilon') \rho_f(\epsilon + \epsilon'), \quad (41)$$

where $\rho_b(\epsilon), \rho_f(\epsilon)$ are spectral functions of the b, f operators, respectively, and the local partition function Z_f is given as

$$Z_f = \int d\epsilon e^{-\beta\epsilon} [\rho_b(\epsilon) + N\rho_f(\epsilon)]. \quad (42)$$

C. Current-voltage relation

The current operator can be derived from the continuity equation $\partial(ed_\sigma^\dagger d_\sigma)/\partial t + \hat{I}_{L\sigma} + \hat{I}_{R\sigma} = 0$. The current operator through the left- and right-reservoirs are obtained as

$$\begin{aligned} \hat{I}_{\alpha\sigma} &= \frac{iet}{\sqrt{\Omega}} \sum_k (c_{\alpha k\sigma}^\dagger d_\sigma - d_\sigma^\dagger c_{\alpha k\sigma}) \\ &= \frac{iet}{\sqrt{\Omega}} \sum_k (c_{\alpha k\sigma}^\dagger b^\dagger f_\sigma - b f^\dagger c_{\alpha k\sigma}). \end{aligned} \quad (43)$$

In the steady-state condition, $\langle d_\sigma^\dagger d_\sigma \rangle$ is constant and

$$I_L + I_R = 0 \quad (44)$$

with $I_\alpha = \sum_\sigma \langle \hat{I}_{\alpha\sigma} \rangle$. If we ignore the \hat{Y}_{cc} term in the effective Hamiltonian as in the previous section, we violate the symmetry condition Eq. (44) as follows. Without the \hat{Y}_{cc} term in $\hat{\mathcal{H}}$, the expectation value of operators appearing in Eq. (43) can be expressed in the finite-temperature Green functions as

$$\frac{it}{\sqrt{\Omega}} \sum_k \langle b f_\sigma^\dagger c_{\alpha k\sigma} \rangle = it^2 \frac{1}{\beta} \sum_{\omega_n} \frac{1}{\Omega} \sum_k \frac{\mathcal{G}_d(i\omega_n)}{i\omega_n - \epsilon_{\alpha k} + \alpha\Phi/2}, \quad (45)$$

where the QD-Green function Eq. (40) has been analytically continued to the imaginary Matsubara frequencies, $i\omega_n = i(2n+1)\pi/\beta$ at integer n . The on-site Green function $\mathcal{G}_d(i\omega_n)$ is independent of the reservoir index α . As discussed in the previous section, the tunneling from the source reservoir is dominated by the electron-hopping, $d^1 \rightarrow d^2$, while the tunneling from the drain reservoir is dominated by the hole-hopping, $d^1 \rightarrow d^0$. Therefore, the modified tunneling in the source and drain-hybridization do not have the same values of at a given energy (See FIG. 4) and the expectation value computed

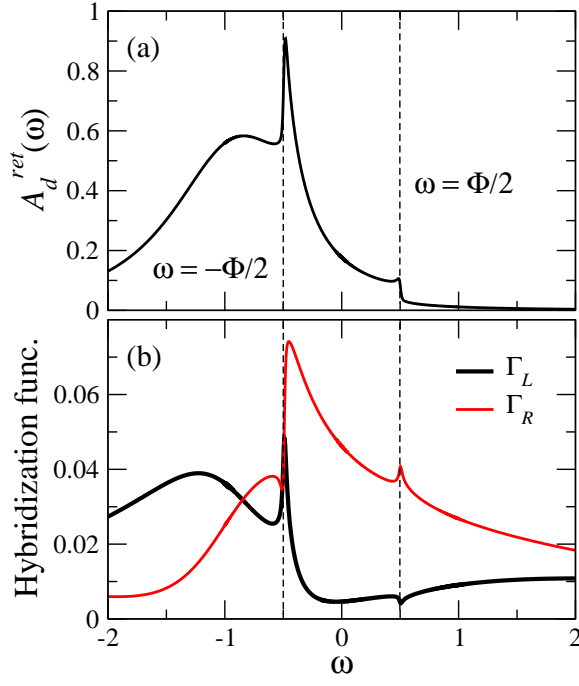


FIG. 4: Spectral function of the retarded Green function for the quantum dot site and the hybridization function from the left- and right-reservoir. The bias Φ is set to 1, $t_L = t_R = 0.48$ and $\beta = 1/T = 160$. The Fermi energy positions for the left ($\omega = \Phi/2$) and the right ($\omega = -\Phi/2$) reservoirs are marked by dashed lines.

from Eq. (45) does not satisfy the charge conservation, Eq. (44).

Physically, it is no surprise that the \hat{Y}_{cc} term is crucial for the current. \hat{Y}_{cc} has the direct coupling between the source and drain reservoirs driven by the bias and has the effect of closing the circuit. Furthermore, phase factors in the coupling act as *current battery* which forces a net current from the source to drain through the quantum dot.

To restore the $L - R$ symmetry, off-diagonal Green functions for conduction electrons $G_{qq'}^0(i\omega_n)$, resulting from \hat{Y}_{cc} , has to be considered in Eq. (45),

$$\begin{aligned} & \frac{it}{\sqrt{\Omega}} \sum_k \langle b f_{\sigma}^{\dagger} c_{\alpha k \sigma} \rangle \\ &= it^2 \frac{1}{\beta} \sum_{\omega_n} \frac{1}{\Omega} \sum_{qq'} G_{qq'}^0(i\omega_n) \mathcal{G}_d(i\omega_n). \end{aligned} \quad (46)$$

Here the conduction electron Green function $G_{qq'}^0(i\omega_n)$ is a propagator in the so-called ‘cavity’ Hamiltonian²¹, where the QD site and its tunneling to the reservoirs are removed from the full Hamiltonian $\hat{\mathcal{H}}$. It should be emphasized that since the bias operator \hat{Y} is built upon the correlated scattering states, even the ‘cavity’ part of the Hamiltonian has correlation effects.

Recalling that much of the correlations effects are already present in the full Green function $g_d(\epsilon)$ in the coef-

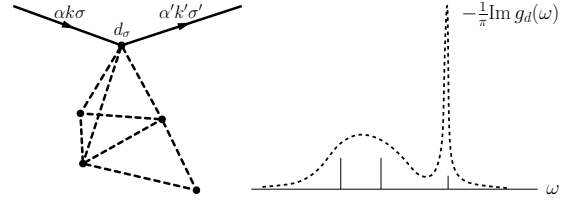


FIG. 5: Coupling between the continuum states in $\hat{H} - \hat{Y}$ is reconstructed by introducing a QD cluster and fitting the QD Green function $g_d(\omega)$.

ficient of the scattered wave [third term in Eq. (31)], we approximate Eq (31), in analogy to the non-interacting scattering state, as

$$\tilde{\psi}_{q\sigma}^{\dagger} = c_{q\sigma}^{\dagger} + \frac{t_{\alpha}}{\sqrt{\Omega}} g_d(\epsilon_q) d_{\sigma}^{\dagger} + \frac{1}{\Omega} \sum_{q'} \frac{t_{\alpha} t_{\alpha'} g_d(\epsilon_q)}{\epsilon_q - \epsilon_{q'} + i\eta} c_{q'\sigma}^{\dagger}, \quad (47)$$

which amount to replacing the factor $(\delta_{\sigma\sigma'} + b^{\dagger} b \delta_{\sigma\sigma'} - f_{\sigma'}^{\dagger} f_{\sigma}^{\dagger})$ by $\delta_{\sigma\sigma'}$. As discussed at the end of Section III-A, $(\delta_{\sigma\sigma'} + b^{\dagger} b \delta_{\sigma\sigma'} - f_{\sigma'}^{\dagger} f_{\sigma}^{\dagger}) = \delta_{\sigma\sigma'}$ without spin-flip scattering.

We now obtain a simple expression for the off-diagonal Green function $G_{qq'}^0(i\omega_n)$ over the ‘cavity’ Hamiltonian based on the non-interacting scattering state operators $\tilde{\psi}_{q\sigma}^{\dagger}$ using the following trick. The Green function $g_d(\epsilon)$ is fitted by introducing an arbitrary, but finite²² number of discrete levels which couple to the QD site [see FIG. 5(a)]. For example, we prepare a finite cluster QD of arbitrary geometry, with the resulting energy poles distributed under the envelope function given by the spectral function of $g_d(\omega)$, [$= -\pi^{-1} \text{Im} g_d(\omega)$], as depicted in FIG. 5(b). We choose the finite cluster such that the peak positions and their weight match the quasi-particle energies and the renormalization factor. Broad peaks can be fitted by introducing multiple cluster peaks underneath, as sketched in FIG. 5(b). The following derivation does not depend on a particular fitting scheme as long as the fitting can be made accurate.

Then, the effective Hamiltonian

$$\tilde{H} - \tilde{Y} = \sum_{\alpha k \sigma} \left[\epsilon_{\alpha k \sigma} - \frac{\alpha \Phi}{2} \right] \tilde{\psi}_{q\sigma}^{\dagger} \tilde{\psi}_{q\sigma}, \quad (48)$$

can approximate the ‘cavity’ part \hat{Y}_{cc} in the original Hamiltonian Eq. (32). Although the QD parts of $\tilde{H} - \tilde{Y}$ and $\hat{H} - \hat{Y}$ can be quite different, it does not matter as long as we are only concerned with the ‘cavity’ Green functions. Carrying out the similar calculations as detailed in the Appendix of Ref.¹², the $c-d$ Green function defined as

$$\begin{aligned} & \tilde{G}_{Ld}(i\omega_n) \\ &= \left\langle c_{L\sigma} \frac{1}{i\omega_n - \mathcal{L}_{H-Y}} d^{\dagger} \right\rangle + \left\langle d^{\dagger} \frac{1}{i\omega_n + \mathcal{L}_{H-Y}} c_{L\sigma} \right\rangle, \end{aligned} \quad (49)$$

with $c_{L\sigma} = \sqrt{\Omega^{-1}} \sum_k c_{Lk\sigma}$, is given by

$$\begin{aligned} & t_L \left[\tilde{G}_{Ld}(i\omega_n) - \tilde{G}_{dL}(i\omega_n) \right] \\ &= 2i \frac{\Gamma_L \Gamma_R}{\Gamma} [g_d(i\omega_n + \Phi/2) - g_d(i\omega_n - \Phi/2)] \end{aligned}$$

The symmetry between the left and right is now. Similarly, the QD Green function can be expressed as

$$\tilde{G}_d(i\omega_n) = \frac{1}{2} [g_d(i\omega_n + \Phi/2) + g_d(i\omega_n - \Phi/2)]$$

The ‘cavity’ Green function then satisfies the Dyson equation

$$\begin{aligned} & t_L \left[\tilde{G}_{Ld}(i\omega_n) - \tilde{G}_{dL}(i\omega_n) \right] \\ &= t_L t_R [G_{LR}^0(i\omega_n) - G_{RL}^0(i\omega_n)] \tilde{G}_d(i\omega_n) \\ &= 4i \frac{\Gamma_L \Gamma_R}{\Gamma} \frac{g_d(i\omega_n + \Phi/2) - g_d(i\omega_n - \Phi/2)}{g_d(i\omega_n + \Phi/2) + g_d(i\omega_n - \Phi/2)} \tilde{G}_d(i\omega_n) \end{aligned}$$

Finally, after replacing $\tilde{G}_d(i\omega_n)$ in the above equation by the nonequilibrium Green function $\mathcal{G}_d(i\omega_n)$, analytically continued from Eq. (40), the Dyson equation for the full off-diagonal Green functions $G_{Ld}(i\omega_n)$ and $G_{dL}(i\omega_n)$ becomes

$$\begin{aligned} & t_L [G_{Ld}(i\omega_n) - G_{dL}(i\omega_n)] \\ &= 4i \frac{\Gamma_L \Gamma_R}{\Gamma} \frac{g_d(i\omega_n + \Phi/2) - g_d(i\omega_n - \Phi/2)}{g_d(i\omega_n + \Phi/2) + g_d(i\omega_n - \Phi/2)} \mathcal{G}_d(i\omega_n). \end{aligned} \quad (52)$$

From $\langle c_{L\sigma}^\dagger d_\sigma \rangle = -\beta^{-1} \sum_n G_{dL}(i\omega_n)$, the current can be expressed as

$$\begin{aligned} I(\Phi) &= N \frac{ie}{\hbar} t_L [\langle d_\sigma^\dagger c_{L\sigma} \rangle - \langle c_{L\sigma}^\dagger d_\sigma \rangle] \\ &= \frac{4Ne}{\hbar} \frac{\Gamma_L \Gamma_R}{\Gamma \beta} \sum_n \frac{g_d(i\omega_n + \Phi/2) - g_d(i\omega_n - \Phi/2)}{g_d(i\omega_n + \Phi/2) + g_d(i\omega_n - \Phi/2)} \mathcal{G}_d(i\omega_n). \end{aligned} \quad (53)$$

The numerator $g_d(i\omega_n + \Phi/2) - g_d(i\omega_n - \Phi/2)$ acts as an energy window opened between the source-drain chemical potential $\pm\Phi/2$ and the Matsubara summation performs the integration over the window. This expression becomes exact¹² in the non-interacting limit with the non-interacting retarded Green function $g_d^0(z)$ as

$$I_0(\Phi) = \frac{4Ne}{\hbar} \frac{\Gamma_L \Gamma_R}{\Gamma} \frac{1}{\beta} \sum_n \frac{1}{2} [g_d^0(i\omega_n + \Phi/2) - g_d^0(i\omega_n - \Phi/2)]. \quad (54)$$

IV. RESULTS

We first discuss the retarded Green function of the quantum dot, $g_d(\epsilon)$, which appear in the expression for the scattering state operator $\psi_{\alpha k \sigma}^\dagger$, Eq. (31). FIG. 4(a) shows the spectral function, $-\pi^{-1} \text{Im} g_d(\omega)$, at the unit bias $\Phi = 1$ with tunneling parameters $t_L = t_R = 0.48$

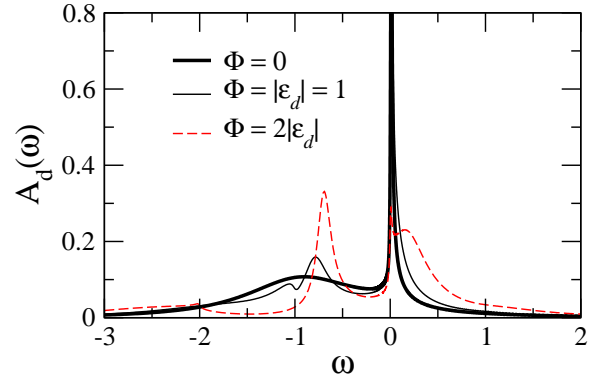


FIG. 6: Spectral function of the thermal Green function with $\hat{H} - \hat{Y}$ as the time-evolution generator. The bias Φ is set to 1, $t_L = t_R = 0.48$ and $\beta = 1/T = 160$.

and the inverse temperature $\beta = 1/T = 1/160$. Throughout the paper, the half-bandwidth D of the Lorentzian DOS of the reservoirs is fixed at $D = 4$. Singular peaks, developed at frequencies $\omega = \Phi/2, -\Phi/2$, correspond to the Fermi levels of the left and right reservoirs, respectively. As the chemical potential of the drain is lowered by $\Phi/2$, the ionization energy of removing one electron from the QD ($E = \epsilon_d$) to the Fermi level of the drain ($E = -\Phi/2$) is reduced to $\Delta E = |\epsilon_d| - \Phi/2$. Therefore a strong Kondo resonance forms on the electrons coming from the right-hand-side continuum at $\omega = -\Phi/2$. Similarly, the resonance formed from the left reservoir produces a much suppressed resonance at $\omega = \Phi/2$.

The resulting hybridization Eq. (39) due to the left and right reservoirs is plotted in FIG. 4(b). As discussed below Eq. (39), the hybridization to the source (L) reservoir has strong intensity at low energy with a strong peak at $\omega = -\Phi/2$ while it is suppressed at high energy with depleted intensity at $\omega = +\Phi/2$. The hybridization to the drain reservoir shows the opposite behavior.

The $I - V$ curves for the parameter set $N = 5$, $\epsilon_d = -1$, $t_{L,R} = 0.48$ in the Kondo regime are shown in FIG. 7(a) at different inverse temperatures $1/T$. For all the tested parameter sets, the current monotonically increases with the bias. The differential conductance $dI/d\Phi$ in (b) shows three distinct features: Kondo peak, inelastic current peak at $\Phi = |\epsilon_d|$ and a very broad inelastic current at high bias.

The Kondo peak, often referred to as the anomalous conductance peak, is the hall-mark of strongly correlated transport. We emphasize that the Kondo peak arises from the combination of the nonequilibrium Green function $\mathcal{G}_d(i\omega)$ and the retarded Green function $g_d(i\omega \pm \Phi/2)$ with the strong correlation effects present in both Green functions [see Eq. (53)]. The conductance $G(\Phi) [= e dI/d\Phi]$ is normalized to the unitary limit $G_0 = Ne^2/h$ with the local degeneracy N .

To discuss the main conclusion and the limitations of this work, we present in FIG. 8 comparisons of the results with other approaches. First, to show that the strong

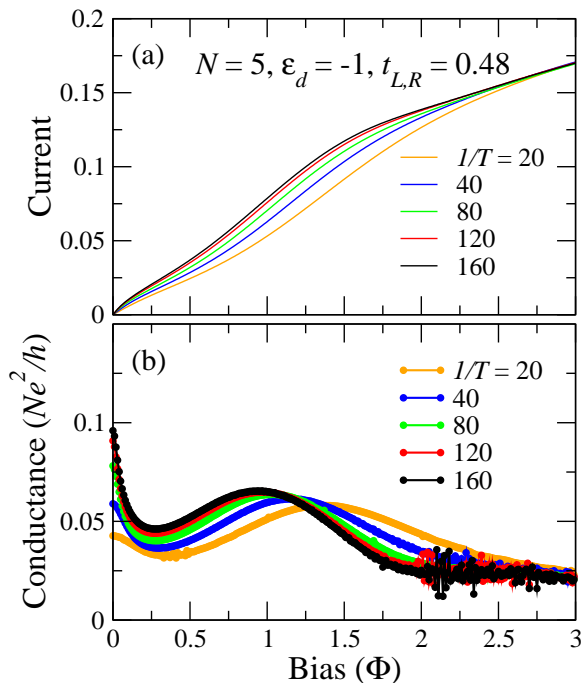


FIG. 7: (a) $I - V$ curves (current in arbitrary unit) in the Kondo regime. (b) Conductance $G(\Phi) = e dI/d\Phi$ normalized to the unitary limit Ne^2/h (with N the degeneracy in the Anderson model). Three peaks correspond to the Kondo resonance, inelastic transport via the charge excitation of the QD at $\Phi = |\epsilon_d|$, and a broad background of inelastic transport of incoherent multiple charge excitations on the QD.

correlation effects should be included at the level of the effective Hamiltonian $\hat{H} - \hat{Y}$, the logarithmic singularity in Eq. (27) is turned off by replacing the Fermi-Dirac factor $f_\alpha(\epsilon)$ by one. The resulting $I - V$ characteristics (dashed line in (a)) does not have the Kondo peak. It is clear that even though the Kondo peak is present in the nonequilibrium Green function $\mathcal{G}_d(\epsilon)$, its absence in the retarded Green function $g_d(\epsilon)$ and therefore in \hat{Y} , leads to no zero-bias conductance peak. This proves that the strong correlation effects in the bias operator \hat{Y} are essential to build correct steady-state nonequilibrium ensemble. Furthermore, at large bias $\Phi \sim 2|\epsilon_f|$, not only is the broad spectrum of inelastic transport missing but also the differential conductance becomes negative. This underestimation of current is due to that the ionization spectrum of the source reservoir at energy $\Phi/2 + \epsilon_d$ and that of the drain at energy $-\Phi/2 + \epsilon_d$ have reduced overlap. However, proper inclusion of the retarded self-energy term compensates the reduced overlap through a strong amplitude in the d^0 -configuration which mediates the inelastic tunneling. (see the strong spectra at $\omega > 0$ for $\Phi = 2|\epsilon_d|$ in FIG. 6).

Since the Friedel-Langreth Fermi-liquid relation of the Anderson model has the QD spectral function at zero frequency $\rho(0) = (1/\pi\Gamma) \sin^2(\pi n_d/N)^{23}$ in the infinite- U

limit, the zero-bias conductance becomes

$$G(\Phi = 0) = \frac{Ne^2}{h} \sin^2\left(\frac{\pi n_d}{N}\right). \quad (55)$$

Using the typical value of $n_d = 0.9$ in these calculations, we get $G(\Phi = 0) \approx 0.29(Ne^2/h)$, about 34% larger than the values shown in FIG. 7. Even though this work shows that the correlation effects included in \hat{Y} produces strongly correlated nonequilibrium ensemble, the discrepancy of the zero-bias conductance is problematic. This is due to the different approximations used to calculate separately the retarded Green function $g_d(\omega)$ in the scattering state operator Eq. (26), and the nonequilibrium Green function $\mathcal{G}_d(\omega)$ Eqs. (35,36) within the NCA. Comparing the sharpness of the Kondo peaks in the FIGs. 4 and 6, we can see that the correlation effects in the retarded self-energy Eq. (26) have been significantly underestimated. In evaluating the current, Eq. (53), the peaks in the two Green functions get convoluted in the Matsubara sum and the over-broadened peak in $g_d(\omega)$ has the effect of smearing out the sharp Kondo peak in $\mathcal{G}_d(\omega)$, leading to the underestimated zero-bias conductance.

It should be emphasized that this shortcoming is due to the inconsistent approximations in the two Green functions, $g_d(\omega)$ and $\mathcal{G}_d(\omega)$, not the mapping of nonequilibrium itself. If the same approximation had been used for the both Green functions, for instance by using the NCA summation scheme (see FIG. 3) for the self-energy in the scattering state operator (see FIG. 2), the zero-bias conductance should have been correct. As proved in Appendix C, the mapping of nonequilibrium produces the correct limit of the zero-bias conductance. Furthermore, as will be discussed in Section V, we develop an algorithm with one Green function and the above problem will disappear.

The central peak at $\Phi = |\epsilon_d|$ in FIG. 7(b) is due to the inelastic transport via charge excitation. Analogous to the one-phonon inelastic process in the electron-phonon coupled QDs¹², electrons tunneling from the source to the drain electrode lose energy of the voltage drop ($\sim \Phi$) while creating charge excitation on the QD with the ionization energy $\sim |\epsilon_d|$.

The spectral function (FIG. 6) at $\Phi = 0$ has a Kondo peak near the chemical potential and the ionization energy peak at $\omega = \epsilon_d$. If we naively expect that the current is proportional to the integral of the zero-bias spectral function between the source-drain chemical potentials, the single-charge ionization process would result in an incorrect conductance peak at $\Phi = 2|\epsilon_d|$, since we model that the source/drain Fermi levels are displaced by $\pm\Phi/2$ with respect to the QD levels. The current calculated by assuming a rigid spectral function $I_{\text{rigid}} \propto \int d\omega \rho_d(\omega, \Phi = 0)[f(\omega - \Phi/2) - f(\omega + \Phi/2)]$, plotted as thin lines in FIG. 8(b), does not show the inelastic peak at $\Phi = |\epsilon_d|$.

The broad background of inelastic transport is due to the strong amplitude of d^0 configuration as noted above. At such high bias, the system is out of the Kondo regime,

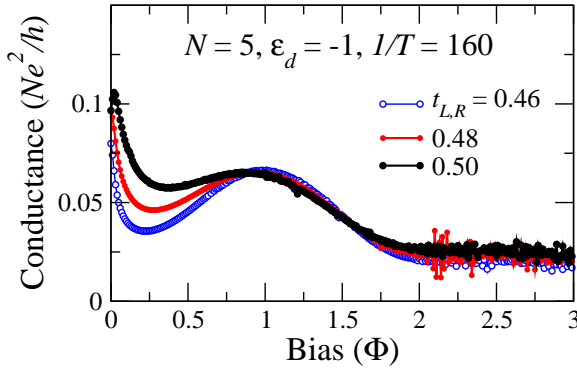
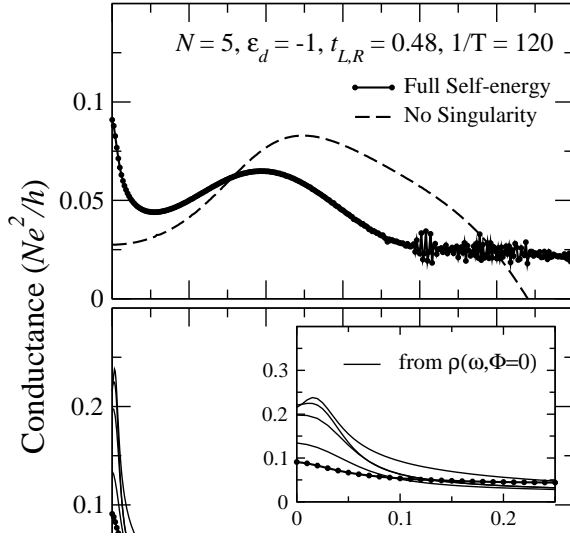


FIG. 9: Normalized conductance to the unitary limit with and without the strong correlation effects in the bias operator \hat{Y} . To turn off the correlation effect in \hat{Y} , the logarithmic singularity is suppressed by replacing the Fermi-Dirac function in Eq. (27). The $I-V$ curve without the correlation effects does not produce the Kondo peak in the conductance.

as can be inferred from the strong spectral weight in the positive frequency ($d^1 \rightarrow d^0$) at $\Phi = 2|\epsilon_d|$ in FIG. 6. Despite the noise in the conductance due to the numerical differentiation at high bias, the trend of increasing intensity of the inelastic transport with the tunneling parameter (see FIG. 9) agrees with the above observation. We

note that the infinite- U approximation becomes increasingly unreliable at high bias since the strong electron-channel of the current-influx to the QD ($d^1 \rightarrow d^2$) is precluded.

Finally, FIG. 9 presents differential conductance as the tunneling parameter is changed. As the tunneling increases, the Kondo resonance becomes stronger and results in pronounced zero-bias anomaly peaks. Since the Kondo peak is shifted to the positive frequency from the Fermi energy by the Kondo temperature, the conductance peak moves from zero to finite bias.

V. SELF-CONSISTENT ALGORITHM

It became clear from the above analysis that the strong correlation effects should be present in the boundary condition. The main problem in the above approach arose from the fact that the nonequilibrium ensemble and the time-evolution are governed by two different operators, $\hat{H}-\hat{Y}$ and \hat{H} . Therefore, to generalize the above method, it is essential to unify the two Hamiltonians with a consistent approximation to solve the generalized impurity model. In this section we propose a practical algorithm to solve this problem.

We start from the observation that the scattering state operators, being eigen-operators of Hamiltonian, also serve as the basis for building the bias operator. The Lippmann-Schwinger equation Eq. (1) is equivalent to the equation of motion,

$$(\epsilon_{\alpha k} - \mathcal{L} + i\eta)\psi_{\alpha k \sigma}^\dagger = i\eta c_{\alpha k \sigma}^\dagger. \quad (56)$$

From the anti-commutation relation Eq. (2), we have

$$\mathcal{L}_Y \psi_{\alpha k \sigma}^\dagger = [\hat{Y}, \psi_{\alpha k \sigma}^\dagger] = \frac{\alpha \Phi}{2} \psi_{\alpha k \sigma}^\dagger. \quad (57)$$

Combining the above two equations, we have a new equation of motion

$$(\epsilon_{\alpha k} - \frac{\alpha \Phi}{2} - \mathcal{L}_{H-Y} + i\eta)\psi_{\alpha k \sigma}^\dagger = i\eta c_{\alpha k \sigma}^\dagger, \quad (58)$$

which is equivalent to the scattering state equation

$$\psi_{\alpha k \sigma}^\dagger = c_{\alpha k \sigma}^\dagger + \frac{1}{\epsilon_{\alpha k} - \alpha \Phi/2 - \mathcal{L}_{H-Y} + i\eta} \mathcal{L}'_V c_{\alpha k \sigma}^\dagger. \quad (59)$$

We now have only one Green function, propagating with the effective Hamiltonian $\hat{H}-\hat{Y}$. The complication is the new tunneling interaction in \mathcal{L}'_V which is modified by the correlation terms in \hat{Y} . However this effect becomes the second order effect since the energy denominator in the Green function has the main strong correlation effects in the modified hybridization function in \hat{Y} , Eq. (39) as considered in the previous section. Furthermore, in the small bias limit where the strong correlation effects are strongest, the correction in \mathcal{L}'_V is proportional to the bias Φ and $\mathcal{L}'_V \approx \mathcal{L}_V$ becomes a good approximation.

Therefore, we propose the following self-consistent algorithm.

- (i) Start from an approximate \hat{Y} , for example from the non-interacting resonant level model¹².
- (ii) Solve $\hat{H} - \hat{Y}$ for the retarded QD Green function $G_d^{\text{ret}}(\omega)$.
- (iii) Approximate $\mathcal{L}'_V = \mathcal{L}_V$ and construct the new bias operator ψ^\dagger using the quasi-particle approximation, Eq. (31), and consequently \hat{Y} with the modified hybridization function given by $G_d^{\text{ret}}(\omega)$ [see Eq. (39)].
- (iv) Go back to the step (i) until it converges.

In this scheme we have a single Green function and the problems arising from two Green functions, such as the underestimated zero-bias conductance, will not occur.

VI. CONCLUSION

We have developed a procedure of mapping a strongly correlated steady-state nonequilibrium to an effective equilibrium. The anti-commutation and completeness relations of the scattering state operators are derived in the interacting limit and the bias operator has been rewritten in a physically appealing form. The mapping of nonequilibrium in the zero-bias limit has been shown to produce the correct linear-response theory.

In the example of the infinite- U Anderson impurity Hamiltonian, as a model for Kondo dot systems, we have derived and analyzed the scattering state operators as the basis for the statistical operator which accounts for the nonequilibrium boundary condition. The strong correlation effects should be included at the Hamiltonian level in the statistical bias operator \hat{Y} to produce the zero-bias Kondo anomaly. The current-voltage relation has been calculated using the equilibrium diagrammatic technique.

Despite the growing understanding of the nonequilibrium ensemble, there are issues to be resolved for this method to be readily applicable to general Hamiltonians. To this end, we have developed a self-consistent algorithm with one kind of Green functions by exploiting the property of the scattering state operators as eigenoperators simultaneously to the Hamiltonian and the bias operators.

The formulation of nonequilibrium steady-state through a mapping to an effective equilibrium not only provides an alternative way of understanding the nonequilibrium, but also can solve various boundary condition problems which are otherwise hard to formulate. For instance, thermal boundary condition, such as thermo-electric effects under a finite temperature difference between reservoirs, can be described quite naturally in the scattering state basis.

One other interesting area is the electron transport with interactions with classical variables which are then self-consistently controlled by the transport, in the sense of the Felicov-Kimball model²⁴. Electron transport

through a chain immersed in a dielectric medium or conduction through fluctuating (classical) spin distributions would be such examples. Since non-interacting scattering states can be written down exactly and the *Boltzmann factors* are now given in a definite expression $\exp[-\beta(\hat{H} - \hat{Y})]$, we can study transport physics in such regime with the current level of formulation.

Acknowledgments

I thank helpful discussions with Natan Andrei, Pankaj Mehta, Eran Lebanon, Michael Fuda and Lingyin Zhu. I acknowledge support from the National Science Foundation DMR-0426826.

APPENDIX A: PROOF OF $\{\psi_r^\dagger, \psi_s\} = \delta_{rs}$.

In the following discussion, we will consider the Hamiltonian with the interaction present only in the QD, such that $\mathcal{L}_V c_s^\dagger = (t/\sqrt{\Omega})d^\dagger$ where \mathcal{L}_V includes the tunneling and many-body interaction terms. For simplicity, we use the subscript s to denote collectively the reservoir and continuum indices (α, k) and suppress the spin index in the following. The Lippmann-Schwinger Eq. (1) becomes

$$\psi_r^\dagger = c_r^\dagger + \frac{t_r}{\sqrt{\Omega}} \frac{1}{\epsilon_r - \mathcal{L} + i\eta} d^\dagger \quad (\text{A1})$$

$$\psi_s = c_s + \frac{t_s}{\sqrt{\Omega}} \frac{1}{\epsilon_s + \mathcal{L} - i\eta} d, \quad (\text{A2})$$

where we have used the relation $(\mathcal{L}A)^\dagger = (HA - AH)^\dagger = A^\dagger H - HA^\dagger = -\mathcal{L}A^\dagger$. We write

$$\{\psi_r^\dagger, \psi_s\} = \delta_{rs} + \hat{\Delta}_{rs}, \quad (\text{A3})$$

with

$$\begin{aligned} \hat{\Delta}_{rs} = & \left\{ \frac{t_r/\sqrt{\Omega}}{\epsilon_r - \mathcal{L} + i\eta} d^\dagger, c_s \right\} + \left\{ c_r^\dagger, \frac{t_s/\sqrt{\Omega}}{\epsilon_s + \mathcal{L} - i\eta} d \right\} \\ & + \frac{t_r t_s}{\Omega} \left\{ \frac{1}{\epsilon_r - \mathcal{L} + i\eta} d^\dagger, \frac{1}{\epsilon_s + \mathcal{L} - i\eta} d \right\}. \end{aligned} \quad (\text{A4})$$

From the relations such as

$$\begin{aligned} & (\epsilon_r - \epsilon_s - \mathcal{L} + i\eta) \left[\left(\frac{1}{\epsilon_r - \mathcal{L} + i\eta} d^\dagger \right) c_s \right] \\ & = d^\dagger c_s + \frac{t_s}{\sqrt{\Omega}} \left(\frac{1}{\epsilon_r - \mathcal{L} + i\eta} d^\dagger \right) d, \end{aligned} \quad (\text{A5})$$

$\hat{\Delta}_{rs}$ can be written as

$$\begin{aligned} \hat{\Delta}_{rs} = & \frac{t_r t_s}{\Omega} \left[\frac{1}{\epsilon_r - \epsilon_s - \mathcal{L} + i\eta} \left\{ \frac{1}{\epsilon_r - \mathcal{L} + i\eta} d^\dagger, d \right\} \right. \\ & - \frac{1}{\epsilon_r - \epsilon_s - \mathcal{L} + i\eta} \left\{ d^\dagger, \frac{1}{\epsilon_s + \mathcal{L} - i\eta} d \right\} \\ & \left. + \left\{ \frac{1}{\epsilon_r - \mathcal{L} + i\eta} d^\dagger, \frac{1}{\epsilon_s + \mathcal{L} - i\eta} d \right\} \right]. \end{aligned} \quad (\text{A6})$$

Here we have used the relations $\{d^\dagger, c_s\} = 0$ and $\mathcal{L}(\hat{A}\hat{B}) = (\mathcal{L}\hat{A})\hat{B} + \hat{A}(\mathcal{L}\hat{B})$. The last term in the previous equation can be rewritten as

$$\begin{aligned} & \left\{ \frac{1}{\epsilon_r - \mathcal{L} + i\eta} d^\dagger, \frac{1}{\epsilon_s + \mathcal{L} - i\eta} d \right\} \\ &= \frac{-1}{\epsilon_r - \epsilon_s - \mathcal{L} + 2i\eta} \\ & \times \left[\left\{ \frac{1}{\epsilon_r - \mathcal{L} + i\eta} d^\dagger, d \right\} - \left\{ d^\dagger, \frac{1}{\epsilon_s + \mathcal{L} - i\eta} d \right\} \right], \end{aligned} \quad (\text{A7})$$

which can be easily verified by multiplying $(\epsilon_r - \epsilon_s - \mathcal{L} + 2i\eta)$ to the both sides of the above equation. The first two terms in Eq. (A6) are canceled by the third term in the $\eta \rightarrow 0$ limit, $\Delta_{rs} = 0$.²⁵ Finally, we have the desired relation

$$\{\psi_r^\dagger, \psi_s\} = \delta_{rs}. \quad (\text{A8})$$

which corresponds to the isometry of the Møller operator in the S -matrix formalism¹⁴.

APPENDIX B: BOUNDARY CONDITION \hat{Y} IN TERMS OF CURRENT OPERATOR

Following similar steps considered in deriving the commutation relation, we can reduce the bias operator \hat{Y} into a convenient form in terms of current operators. We write \hat{Y} as

$$\hat{Y} = \frac{\Phi}{2} (\hat{\mathcal{N}}_L - \mathcal{N}_R), \text{ with } \hat{\mathcal{N}}_\alpha = \sum_k \psi_{\alpha k}^\dagger \psi_{\alpha k}. \quad (\text{B1})$$

Similar steps leading to Eq. (A4) give

$$\begin{aligned} & \psi_{\alpha k}^\dagger \psi_{\alpha k} = c_{\alpha k}^\dagger c_{\alpha k} \\ & + \frac{t_{\alpha k}}{\sqrt{\Omega}} \left[\left(\frac{1}{\epsilon_{\alpha k} - \mathcal{L} + i\eta} d^\dagger \right) c_{\alpha k} + c_{\alpha k}^\dagger \left(\frac{1}{\epsilon_{\alpha k} + \mathcal{L} - i\eta} d \right) \right] \\ & + \frac{t_{\alpha k}^2}{\Omega} \left(\frac{1}{\epsilon_{\alpha k} - \mathcal{L} + i\eta} d^\dagger \right) \left(\frac{1}{\epsilon_{\alpha k} + \mathcal{L} - i\eta} d \right). \end{aligned} \quad (\text{B2})$$

The second and third terms can be rewritten as Eq. (A5) with $\epsilon_r = \epsilon_s = \epsilon_{\alpha k}$:

$$\begin{aligned} & \left(\frac{1}{\epsilon_{\alpha k} - \mathcal{L} + i\eta} d^\dagger \right) c_{\alpha k} \\ &= \frac{1}{-\mathcal{L} + i\eta} \left(d^\dagger c_{\alpha k} + \frac{t_{\alpha k}/\sqrt{\Omega}}{\epsilon_{\alpha k} - \mathcal{L} + i\eta} d^\dagger \cdot d \right). \end{aligned} \quad (\text{B3})$$

The second term in Eq. (B3) is canceled by the last term of the Eq. (B2) in the $\eta \rightarrow 0$ limit,

$$\begin{aligned} & \left(\frac{1}{\epsilon_{\alpha k} - \mathcal{L} + i\eta} d^\dagger \right) \left(\frac{1}{\epsilon_{\alpha k} + \mathcal{L} - i\eta} d \right) \\ &= \frac{1}{\mathcal{L} - 2i\eta} \left[\left(\frac{1}{\epsilon_{\alpha k} - \mathcal{L} + i\eta} d^\dagger \right) d - d^\dagger \left(\frac{1}{\epsilon_{\alpha k} + \mathcal{L} - i\eta} d \right) \right]. \end{aligned} \quad (\text{B4})$$

Following the same steps as in the previous Appendix, we have

$$\psi_{\alpha k}^\dagger \psi_{\alpha k} = c_{\alpha k}^\dagger c_{\alpha k} + \frac{t_{\alpha k}}{\sqrt{\Omega}} \frac{1}{-\mathcal{L} + i\eta} (d^\dagger c_{\alpha k} - c_{\alpha k}^\dagger d). \quad (\text{B5})$$

Therefore the bias operator can be expressed in a simple form as

$$\hat{Y} = \Phi \left[\hat{y}_0 + \frac{1/2}{-\mathcal{L} + i\eta} (d^\dagger \tilde{c}_L - \tilde{c}_L^\dagger d - d^\dagger \tilde{c}_R + \tilde{c}_R^\dagger d) \right], \quad (\text{B6})$$

with $\hat{y}_0 = \frac{1}{2} \sum_k (c_{Lk}^\dagger c_{Lk} - c_{Rk}^\dagger c_{Rk})$ and $\tilde{c}_\alpha^\dagger = \Omega^{-1/2} \sum_k t_{\alpha k} c_{\alpha k}^\dagger$. Defining the source-to-drain electric current as

$$\begin{aligned} \hat{I} &= \frac{1}{2} (\hat{I}_L - \hat{I}_R) \\ &= \frac{ie}{2} (d^\dagger \tilde{c}_L - \tilde{c}_L^\dagger d - d^\dagger \tilde{c}_R + \tilde{c}_R^\dagger d), \end{aligned} \quad (\text{B7})$$

we have the bias operator in terms of the current operator as,

$$\hat{Y} \equiv \Phi \hat{y} = \Phi \left[\hat{y}_0 - \frac{1}{e} \frac{i}{-\mathcal{L} + i\eta} \hat{I} \right]. \quad (\text{B8})$$

Or, alternatively, by making use of $\mathcal{L}_V(c_{\alpha k}^\dagger c_{\alpha k}) = (t_{\alpha k}/\sqrt{\Omega})(d^\dagger c_{\alpha k} - c_{\alpha k}^\dagger d)$ for Hamiltonians with only local interactions on the quantum dots,

$$\hat{Y} = \Phi \left[\hat{y}_0 + \frac{1}{-\mathcal{L} + i\eta} \mathcal{L}_V \hat{y}_0 \right], \quad (\text{B9})$$

which is equivalent to the equation of motion for the bias operator \hat{Y} , $[\hat{H}, \hat{Y}] = i\eta(\hat{Y} - \hat{Y}_0)$, in Hershfield's paper¹⁰.

APPENDIX C: DERIVATION OF ZERO-BIAS LIMIT CONDUCTANCE

In the zero-bias limit, the present formulation via mapping of nonequilibrium should recover the linear response formula with the conductance given by the current-current correlation function. With the expression derived in the previous section, one can prove this as follows. The current is evaluated via the thermal average taken over the nonequilibrium ensemble,

$$I = Z^{-1} \text{Tr} \left(e^{-\beta(\hat{H} - \hat{Y})} \hat{I} \right), \text{ with } Z = \text{Tr} e^{-\beta(\hat{H} - \hat{Y})}. \quad (\text{C1})$$

By differentiating the current by the bias Φ in $\hat{Y} = \Phi \hat{y}$ about the zero-bias limit, we obtain the expression of the conductance in terms of the imaginary-time correlation function,

$$G_0 = e \frac{\partial I}{\partial \Phi} = e \int_0^\beta d\tau \langle \hat{y}(\tau) \hat{I}(0) \rangle \text{ with } \hat{y}(\tau) = e^{\tau \mathcal{L}} \hat{y}, \quad (\text{C2})$$

where we have used the relation $\langle \hat{I} \rangle = 0$.

The \hat{y} term has two contributions, as in Eq. (B8), from \hat{y}_0 and \hat{I} . It can be shown that the contribution from \hat{y}_0 can be dropped, as follows. For the sake of argument, we express the Hamiltonian \hat{H} in terms of real numbers. Since the expectation values such as $\langle \hat{y}_0 d^\dagger c_L \rangle$ are all real numbers, they have no contributions in $\langle \hat{y}_0 \hat{I} \rangle_0$ according to Eq. (B7). Therefore we have

$$G_0 = - \int_0^\beta d\tau \langle \hat{I}_1(\tau) \hat{I}(0) \rangle, \text{ with } \hat{I}_1 = \frac{i}{-\mathcal{L} + i\eta} \hat{I}. \quad (\text{C3})$$

Analytically continuing the above integral from the imaginary-time to the real-time integral, we have the fluctuation-dissipation theorem

$$G_0 = \int_{-\infty}^{\infty} dt \chi(t) \text{ with } \chi(t) = -i\theta(-t) \langle [\hat{I}(0), \hat{I}_1(t)] \rangle. \quad (\text{C4})$$

Fourier transform of the response function $\chi(t)$ becomes

$$\begin{aligned} \chi(\omega) &= -i \int_{-\infty}^0 dt e^{\eta t + i\omega t} \langle [\hat{I}, e^{i\mathcal{L}t} \hat{I}_1] \rangle \\ &= -i \left\langle \left[\hat{I}, \frac{i}{\omega - \mathcal{L} + i\eta} \frac{i}{-\mathcal{L} + i\eta} \hat{I} \right] \right\rangle. \end{aligned} \quad (\text{C5})$$

From

$$\frac{i}{\omega - \mathcal{L} + i\eta} \frac{i}{-\mathcal{L} + i\eta} = \frac{i}{\omega} \left[\frac{i}{-\mathcal{L} + i\eta} - \frac{i}{\omega - \mathcal{L} + i\eta} \right] \quad (\text{C6})$$

and

$$\text{Re} \left\langle \hat{I} \left(\frac{i}{-\mathcal{L} + i\eta} \hat{I} \right) \right\rangle = \text{Re} \left\langle \left(\frac{i}{-\mathcal{L} + i\eta} \hat{I} \right) \hat{I} \right\rangle, \quad (\text{C7})$$

the response function is written by the current-current response function $\chi_{II}(t) = -i\theta(t) \langle [\hat{I}(t), \hat{I}(0)] \rangle$ as

$$\begin{aligned} \chi(\omega) &= \frac{1}{i\omega} \chi_{II}(\omega) = \frac{1}{i\omega} \left\langle \left[\hat{I}, \frac{1}{\omega - \mathcal{L} + i\eta} \hat{I} \right] \right\rangle \\ &= \frac{1}{i\omega} \int_{-\infty}^0 dt e^{\eta t + i\omega t} (-i) \langle [\hat{I}(0), \hat{I}(t)] \rangle. \end{aligned} \quad (\text{C8})$$

Finally we obtain the zero-bias conductance in terms of the linear response theory in agreement with the Kubo formula,

$$G_0 = \lim_{\omega \rightarrow 0} \chi(\omega) = \lim_{\omega \rightarrow 0} \frac{\chi_{II}(\omega)}{i\omega}. \quad (\text{C9})$$

APPENDIX D: COMPLETENESS OF $\psi_{\alpha k \sigma}^\dagger$

For non-interacting models¹² without bound states, the scattering state operators satisfy a completeness relation

$$\sum_{\alpha k} \psi_{\alpha k \sigma}^\dagger \psi_{\alpha k \sigma} = \sum_{\alpha k} c_{\alpha k \sigma}^\dagger c_{\alpha k \sigma} + d_\sigma^\dagger d_\sigma, \quad (\text{D1})$$

and the Hamiltonian is written as a sum over $\psi_{\alpha k \sigma}$ as

$$\sum_{\alpha k \sigma} \epsilon_{\alpha k} \psi_{\alpha k \sigma}^\dagger \psi_{\alpha k \sigma} = \hat{H}. \quad (\text{D2})$$

For the interacting case, it is not clear at all whether such relations hold when $\psi_{\alpha k \sigma}^\dagger$ is made not only of one-particle creation operators but also of many-particle excitations.

First we assume that the Hamiltonian has many-body interaction \hat{H}' term only on the QD (d_σ) site and it takes the form

$$\begin{aligned} \hat{H} &= \sum_{\alpha k \sigma} \epsilon_{\alpha k} c_{\alpha k}^\dagger c_{\alpha k} + \sum_{\alpha k \sigma} \frac{t_{\alpha k}}{\sqrt{\Omega}} \left(d_\sigma^\dagger c_{\alpha k} + c_{\alpha k}^\dagger d_\sigma \right) \\ &+ \epsilon_d \sum_{\sigma} d_\sigma^\dagger d_\sigma + \hat{H}'(d_\uparrow^\dagger, d_\uparrow, d_\downarrow^\dagger, d_\downarrow). \end{aligned} \quad (\text{D3})$$

We derive corresponding relations for the interacting case starting from Eq. (B5). After summing over the continuum variables on both sides of the equation,

$$\sum_{\alpha k} \psi_{\alpha k}^\dagger \psi_{\alpha k} = \sum_{\alpha k} c_{\alpha k}^\dagger c_{\alpha k} + \sum_{\alpha k} \frac{t_{\alpha k} / \sqrt{\Omega}}{-\mathcal{L} + i\eta} \left(d_\sigma^\dagger c_{\alpha k} - c_{\alpha k}^\dagger d_\sigma \right). \quad (\text{D4})$$

With the Hamiltonian Eq. (D3),

$$\mathcal{L}(d_\sigma^\dagger d_\sigma) = \sum_{\alpha k} \frac{t_{\alpha k}}{\sqrt{\Omega}} \left(c_{\alpha k}^\dagger d_\sigma - d_\sigma^\dagger c_{\alpha k} \right) + \mathcal{L}'(d_\sigma^\dagger d_\sigma). \quad (\text{D5})$$

Substituting this to the previous equation, we have

$$\begin{aligned} \sum_{\alpha k} \psi_{\alpha k}^\dagger \psi_{\alpha k} &= \sum_{\alpha k} c_{\alpha k}^\dagger c_{\alpha k} + \frac{1}{-\mathcal{L} + i\eta} (-\mathcal{L} n_\sigma + \mathcal{L}' n_\sigma) \\ &= \sum_{\alpha k} c_{\alpha k}^\dagger c_{\alpha k} + d_\sigma^\dagger d_\sigma + \frac{1}{-\mathcal{L} + i\eta} \mathcal{L}' n_\sigma \end{aligned} \quad (\text{D6})$$

In the last line we have used that $-\mathcal{L}/(-\mathcal{L} + i\eta) = 1 - i\eta/(-\mathcal{L} + i\eta) \rightarrow 1$ and assumed that there exist no isolated energy eigenstates^{12,15}. If there is an isolated state $|E_0\rangle$ outside the continuum it cannot be constructed by the scattering states. If $n_\sigma = d^\dagger d$ has a finite amplitude of $\psi_0^\dagger \psi_0$, with the creation operator ψ_0^\dagger of the state $|E_0\rangle$, it does not contribute in the k -summation of scattering states, *i.e.* $-\mathcal{L}/(-\mathcal{L} + i\eta) (\psi_0^\dagger \psi_0) = 0$. In other words, the operator $i\eta/(-\mathcal{L} + i\eta)$ projects out the contribution of isolated states in n_σ .

If the interaction is written in terms of d -density operators only, such as the Hubbard Coulomb interaction $\hat{H}' = U n_\uparrow n_\downarrow$, $\mathcal{L}' n_\sigma = 0$. Therefore, we recover Eq. (D1) in the interacting case.

We proceed similarly for Eq. (D2):

$$\begin{aligned} &\sum_{\alpha k} \epsilon_{\alpha k} \psi_{\alpha k \sigma}^\dagger \psi_{\alpha k \sigma} \\ &= \sum_{\alpha k \sigma} \epsilon_{\alpha k} c_{\alpha k}^\dagger c_{\alpha k} + \sum_{\alpha k} \frac{t_{\alpha k} / \sqrt{\Omega}}{-\mathcal{L} + i\eta} \epsilon_{\alpha k} \left(d_\sigma^\dagger c_{\alpha k \sigma} - c_{\alpha k \sigma}^\dagger d_\sigma \right). \end{aligned} \quad (\text{D7})$$

Since $\mathcal{L}c_{\alpha k}^\dagger = \epsilon_{\alpha k}c_{\alpha k\sigma}^\dagger + (t_{\alpha k}/\sqrt{\Omega})d_\sigma^\dagger$,

$$d_\sigma^\dagger(\mathcal{L}c_{\alpha k\sigma}) + (\mathcal{L}c_{\alpha k\sigma}^\dagger)d_\sigma = -\epsilon_{\alpha k}(d_\sigma^\dagger c_{\alpha k\sigma} - c_{\alpha k\sigma}^\dagger d_\sigma), \quad (\text{D8})$$

and

$$\begin{aligned} & d_\sigma^\dagger(\mathcal{L}c_{\alpha k\sigma}) + (\mathcal{L}c_{\alpha k\sigma}^\dagger)d_\sigma \\ &= \mathcal{L}(d_\sigma^\dagger c_{\alpha k\sigma} + c_{\alpha k\sigma}^\dagger d_\sigma) - (\mathcal{L}d_\sigma^\dagger)c_{\alpha k\sigma} - c_{\alpha k\sigma}^\dagger(\mathcal{L}d_\sigma). \end{aligned} \quad (\text{D9})$$

Therefore, Eq. (D7) can be summarized, so far, as

$$\begin{aligned} & \sum_{\alpha k\sigma} \epsilon_{\alpha k} \psi_{\alpha k\sigma}^\dagger \psi_{\alpha k\sigma} \\ &= \sum_{\alpha k\sigma} \epsilon_{\alpha k} c_{\alpha k\sigma}^\dagger c_{\alpha k\sigma} + \sum_{\alpha k\sigma} \frac{t_{\alpha k}}{\sqrt{\Omega}} \left(d_\sigma^\dagger c_{\alpha k\sigma} + c_{\alpha k\sigma}^\dagger d_\sigma \right) \\ &+ \frac{1}{-\mathcal{L} + i\eta} \sum_{\alpha k\sigma} \frac{t_{\alpha k}}{\sqrt{\Omega}} \left[(\mathcal{L}d_\sigma^\dagger)c_{\alpha k\sigma} + c_{\alpha k\sigma}^\dagger(\mathcal{L}d_\sigma) \right]. \end{aligned} \quad (\text{D10})$$

From $\mathcal{L}d_\sigma^\dagger = \sum_{\alpha k}(t_{\alpha k}/\sqrt{\Omega})c_{\alpha k\sigma}^\dagger + \epsilon_d d_\sigma^\dagger + \mathcal{L}'d_\sigma^\dagger$, the last term in the previous equation becomes, before the spin summation is taken,

$$\begin{aligned} & \frac{1}{-\mathcal{L} + i\eta} \sum_{\alpha k} \frac{t_{\alpha k}}{\sqrt{\Omega}} \left[(\mathcal{L}d_\sigma^\dagger)c_{\alpha k\sigma} + c_{\alpha k\sigma}^\dagger(\mathcal{L}d_\sigma) \right] \\ &= \frac{1}{-\mathcal{L} + i\eta} \left[(\mathcal{L}d_\sigma^\dagger)(-\mathcal{L}d_\sigma - \epsilon_d d_\sigma + \mathcal{L}'d_\sigma) \right. \\ & \quad \left. + (\mathcal{L}d_\sigma^\dagger - \epsilon_d d_\sigma^\dagger - \mathcal{L}'d_\sigma^\dagger)(\mathcal{L}d_\sigma) \right] \\ &= \epsilon_d d_\sigma^\dagger d_\sigma + \frac{1}{-\mathcal{L} + i\eta} \left[(\mathcal{L}d_\sigma^\dagger)(\mathcal{L}'d_\sigma) - (\mathcal{L}'d_\sigma^\dagger)(\mathcal{L}d_\sigma) \right]. \end{aligned} \quad (\text{D11})$$

By defining the non-interaction part as \hat{H}_0 we have

$$\begin{aligned} & \sum_{\alpha k\sigma} \epsilon_{\alpha k} \psi_{\alpha k\sigma}^\dagger \psi_{\alpha k\sigma} \\ &= \hat{H}_0 + \frac{1}{-\mathcal{L} + i\eta} \sum_{\sigma} \left[(\mathcal{L}d_\sigma^\dagger)(\mathcal{L}'d_\sigma) - (\mathcal{L}'d_\sigma^\dagger)(\mathcal{L}d_\sigma) \right]. \end{aligned} \quad (\text{D12})$$

If the interaction is the Hubbard on-site Coulomb interaction $\hat{H}' = U n_\sigma n_{\bar{\sigma}}$,

$$\begin{aligned} & -(\mathcal{L}d_\sigma^\dagger)(\mathcal{L}'d_\sigma) + (\mathcal{L}'d_\sigma^\dagger)(\mathcal{L}d_\sigma) \\ &= U(\mathcal{L}d_\sigma^\dagger)n_{\bar{\sigma}}d_\sigma + U n_{\bar{\sigma}}d_\sigma^\dagger(\mathcal{L}d_\sigma) \\ &= U \left[(\mathcal{L}d_\sigma^\dagger)n_{\bar{\sigma}}d_\sigma + d_\sigma^\dagger \{ \mathcal{L}(n_{\bar{\sigma}}d_\sigma) - (\mathcal{L}n_{\bar{\sigma}})d_\sigma \} \right] \\ &= U \left[\mathcal{L}(n_\sigma n_{\bar{\sigma}}) - (\mathcal{L}n_{\bar{\sigma}})n_\sigma \right]. \end{aligned} \quad (\text{D13})$$

Summing over spins, the interaction term becomes

$$U \sum_{\sigma} \left[(\mathcal{L}d_\sigma^\dagger)(\mathcal{L}'d_\sigma) - (\mathcal{L}'d_\sigma^\dagger)(\mathcal{L}d_\sigma) \right] = \mathcal{L}(U n_\sigma n_{\bar{\sigma}}) = \mathcal{L}\hat{H}'. \quad (\text{D14})$$

Finally, we obtain for the Anderson impurity model

$$\sum_{\alpha k\sigma} \epsilon_{\alpha k} \psi_{\alpha k\sigma}^\dagger \psi_{\alpha k\sigma} = \hat{H}_0 + \hat{H}' = \hat{H}, \quad (\text{D15})$$

in the absence of bound states.

-
- ¹ S. Datta, *Electronic Transport in Mesoscopic Systems*, Cambridge University Press, Cambridge UK (1995).
² J. Rammer and H. Smith, Rev. Mod. Phys. **58**, 323 (1986).
³ N. S. Wingreen, K. W. Jacobsen, and J. W. Wilkins, Phys. Rev. Lett. **61**, 1396 (1988); N. S. Wingreen, K. W. Jacobsen, and J. W. Wilkins, Phys. Rev. B **40**, 11834 (1989).
⁴ R. Lake and S. Datta, Phys. Rev. B **45**, 6670 (1992).
⁵ R. Aguado and D. C. Langreth, Phys. Rev. B **67**, 245307 (2003).
⁶ P. Mehta and N. Andrei, cond-mat/0508026 (2005).
⁷ N. Shah and A. Rosch, Phys. Rev. B **73**, 081309 (2006).
⁸ F. Anders and A. Schiller, Phys. Rev. Lett. **95**, 196801 (2006).
⁹ D. N. Zubarev, *Nonequilibrium Statistical Thermodynamics*, Consultants Bureau, New York (1974).
¹⁰ S. Hershfield, Phys. Rev. Lett. **70**, 2134 (1993).
¹¹ A. Schiller and S. Hershfield, Phys. Rev. B **51**, 12896 (1995).
¹² J. E. Han, Phys. Rev. B **73**, 125319 (2006).
¹³ S. M. Cronenwett, T. H. Oosterkamp, L. P. Kouwenhoven, Science **281**, 540 (1998); W. G. van der Wiel, *et al.*, Science **289**, 2105 (2000).
¹⁴ Arno Bohm, *Quantum Mechanics: Foundations and Applications*, Chapter XV, Springer-Verlag, New York (1986).
¹⁵ M. Gell-Mann and M. L. Goldberger, Phys. Rev. **91**, 398

- (1953).
¹⁶ P. Bokes and R. W. Godby, Phys. Rev. B **68**, 125414 (2003).
¹⁷ Eugen Merzbacher, *Quantum Mechanics*, Chapter 21, John Wiley & Sons, New York (1961).
¹⁸ In the narrow band limit or band with a sharp edge, there are localized states which cannot be included in $\psi_{\alpha k\sigma}$. However they do not contribute to \hat{Y} .
¹⁹ P. Coleman, Phys. Rev. B **29**, 3035 (1984).
²⁰ N. E. Bickers, D. L. Cox, and J. W. Wilkins, Phys. Rev. B **36**, 2036 (1987); N. E. Bickers, Rev. Mod. Phys. **59**, 845 (1987).
²¹ A. Georges, G. Kotliar, W. Krauth, and M. J. Rozenberg, Rev. Mod. Phys. **68**, 13 (1996).
²² An infinite cluster acts as another reservoir and the resulting current violates $I_L + I_R = 0$.
²³ K. Yamada, Prog. Theor. Phys. **53**, 970 (1975).
²⁴ J. K. Freericks and V. Zlatic, Rev. Mod. Phys. **75**, 1333 (2003).
²⁵ We set the incoming wave as a wave-packet with finite spread of width $\delta\epsilon_r \sim \eta$ and the $\epsilon_r = \epsilon_s$ condition is understood as an integral over the energy spread, which makes the difference between the 2η and η in the denominator expressions irrelevant. For more detailed discussions, see M. L. Goldberger and K. M. Watson, *Collision Theory*, p.180,

Wiley, New York (1964).